

Possibility for rapid generation of high-pressure phases in single-crystal silicon by fast nanoindentation

This content has been downloaded from IOPscience. Please scroll down to see the full text.

2015 Semicond. Sci. Technol. 30 115001

(<http://iopscience.iop.org/0268-1242/30/11/115001>)

View [the table of contents for this issue](#), or go to the [journal homepage](#) for more

Download details:

IP Address: 131.113.58.246

This content was downloaded on 24/03/2016 at 05:23

Please note that [terms and conditions apply](#).

Possibility for rapid generation of high-pressure phases in single-crystal silicon by fast nanoindentation

Hu Huang and Jiwang Yan

Department of Mechanical Engineering, Keio University, Yokohama 223-8522, Japan

E-mail: yan@mech.keio.ac.jp

Received 17 May 2015, revised 24 August 2015

Accepted for publication 28 August 2015

Published 28 September 2015



CrossMark

Abstract

High-pressure phases of silicon such as Si-XII/Si-III exhibit attractive optical, electrical and chemical properties, but until now, it has been technologically impossible to produce a significant quantity of Si-XII or Si-III. In this study, to explore the possibility of generating high-pressure silicon phases efficiently, comparative nanoindentation experiments were conducted. Effects of the loading rate, unloading rate and maximum indentation load were investigated, and key factors affecting the high-pressure phase formation were identified. A new nanoindentation protocol is proposed that introduces an intermediate holding stage into the unloading process. The resulting end phases under the indent were detected by a laser micro-Raman spectrometer and compared with those formed in conventional nanoindentation. The results indicate that high-pressure phases Si-XII and Si-III were successfully formed during the intermediate holding stage even with a very high loading/unloading rate. This finding demonstrates the possibility of rapid production of high-pressure phases of silicon through fast mechanical loading and unloading.

Keywords: single-crystal silicon, high-pressure phase, nanoindentation, phase transformation, load control

(Some figures may appear in colour only in the online journal)

1. Introduction

Single-crystal silicon is an important substrate material in current scientific research and industrial applications, and has been widely used in semiconductor device fabrication, solar cells, micro-electro-mechanical systems, and so on. To further improve and extend its applications, the electrical, mechanical and chemical properties of silicon are attracting multi-disciplinary attention. Pressure-induced phase transformation behaviors in single-crystal silicon are commonly observed in diamond anvil cell experiments and nanoindentation tests [1–7]. Based on these two experimental methods, metastable polymorphs of silicon have been reported [6, 8–11]. Under pressure ~ 10 GPa during diamond anvil cell tests, diamond-cubic Si (Si-I phase) transforms into a metallic Si-II phase (β -tin structure) whose density is $\sim 22\%$ higher than that of the Si-I phase [11, 12]. With further increase of pressure to ~ 80 GPa, phase transformations into Si-XI, Si-V, Si-VI, Si-

VII, and Si-X occur sequentially [12]. Upon release of pressure, reversible transformations sequentially occur until the Si-II phase is formed. With further pressure release to ~ 9 GPa, the Si-II phase does not transform back to the Si-I phase but transforms into a Si-XII phase with rhombohedral structure [8], which further transforms into a Si-III phase with body-centered cubic structure [6]. The transformation from the Si-II phase to the Si-XII/Si-III phases involves remarkable expansion [11], which is clearly visible in nanoindentation tests [13].

These polymorphs of Si formed during pressure increase/release exhibit attractive mechanical, optical, electrical and chemical properties [14–18]. For example, the Si-XII phase has a narrow bandgap and exhibits greater overlap with the solar spectrum than other silicon phases [15, 16], giving it the potential to improve absorption of the solar spectrum. The Si-III phase is semimetal [19], with potential applications in multiple exciton generation and next-

generation photovoltaics [20]. In addition, the Si-XII/Si-III phases have high resistance to etching in the KOH solution, providing a new maskless patterning method for fabricating nanoscale patterns on Si surfaces [17].

Although these high-pressure phases have attractive properties, producing a significant quantity of Si-XII or Si-III is still a challenge. Thus, exploration of the formation of high-pressure Si phases is undoubtedly important. Much previous research has been done to investigate the effects of various experimental parameters on phase transformations in single-crystal silicon using nanoindentation, such as indentation loads, loading/unloading rates, indenter types and angles, and so on [21–27]. Previous research on Si nanoindentation indicates that phase transformations during unloading are sensitive to the indentation load and loading/unloading rates [22, 23, 27, 28]. A large indentation load and a low loading/unloading rate are preferred to induce the phase transformation from Si-II into Si-XII/Si-III during unloading, leading to a discontinuous displacement burst, namely pop-out in the unloading curve. However, when the indentation load is small and the loading/unloading rate is high, the Si-II phase readily transforms into an amorphous phase (*a*-Si) whose density is also less than the Si-II phase, and thus an elbow is usually observed in the unloading curve. Although some other reasons, such as dislocation, fracture and delamination may also induce discontinuities in load-displacement curves [29], previous research results by *ex/in situ* Raman microspectroscopy [4, 13, 22, 30], cross-sectional transmission electron microscopy (XTEM) [23, 31, 32], and *in situ* electrical characterization [32, 33] demonstrated that discontinuities in nanoindentation unloading curves of Si were directly correlated to phase transformations. Hence, the shape of the unloading curve can be regarded as an indicator for phase transformations [13]. However, so far, there has been little research focusing on how to efficiently produce the high-pressure phases. In this study, we will investigate the key factors affecting the formation of high-pressure phases in nanoindentation of single-crystal silicon, and explore an efficient approach to produce high-pressure phases under high loading and unloading rates.

2. Experimental details

An *n*-type boron-doped single-crystal silicon (100) sample with a resistivity of $2.0 \sim 8.0 \Omega\text{cm}$ was prepared from a wafer. A nanoindentation instrument ENT-1100 (Elionix Inc., Japan) equipped with a Berkovich indenter was used to perform nanoindentation tests. To study the effects of indentation loads and loading/unloading rates on the formation of high-pressure phases, two maximum indentation loads, 30 and 60 mN, and two loading/unloading rates, 1 and 30 mN s^{-1} , were selected. The maximum indentation load was held for 1 s. To distinguish the effects of the loading rate and unloading rate on the formation of high-pressure phases, their values were set to be different for some tests, for example, 30 mN s^{-1} for loading and 1 mN s^{-1} for unloading. To explore the possibility of forming high-pressure phases under

a high loading/unloading rate (30 mN s^{-1}), we introduced an intermediate holding stage during unloading for a period of 20 s at loads of 8 and 16 mN for the maximum indentation loads of 30 and 60 mN, respectively. For statistical analysis, 20 nanoindentation tests were carried out for each experimental condition. Residual phases in the indents after indentation were detected by a laser micro-Raman spectrometer NRS-3000 (JASCO, Tokyo, Japan) with a 532 nm wavelength laser focused to a $\sim 1 \mu\text{m}$ spot size.

3. Results and discussion

Figure 1 presents statistical results of nanoindentation in single-crystal silicon under a maximum indentation load of 30 mN. For various loading/unloading rates, an obvious difference appears. For a loading/unloading rate of 1 mN s^{-1} , pop-out appears 14 times in 20 tests and only 6 tests show elbows in load-displacement curves (figure 1(a)). For a loading/unloading rate of 30 mN s^{-1} , as shown in figure 1(b), no pop-out occurs and all 20 tests show elbows. Similarly, in figure 1(c) where the loading rate is 1 mN s^{-1} and the unloading rate is 30 mN s^{-1} , only elbows occur in all 20 tests without pop-outs. However, when the loading rate is set to 30 mN s^{-1} and the unloading rate is set to 1 mN s^{-1} , pop-outs are observed in 13 tests and elbows in 7 tests (figure 1(d)), similar to the result in figure 1(a).

The results shown in figures 1(a) and (b) agree well with those obtained by previous researchers, i.e., a low loading/unloading rate promotes the occurrence of pop-out while a high loading/unloading rate frequently leads to elbows [22, 23, 27, 28]. However, the individual effects of the loading rate and the unloading rate on the formation of high-pressure phases have not previously been distinguished.

For unloading, the authors of [32, 34] proposed a crystal nucleation and growth mechanism to describe the formation of high-pressure Si-XII/Si-III phases. It is a two-step process. First, some high-pressure phase volumes are randomly nucleated within the Si-II phase at early stages of unloading, and these small volumes serve as seeds for subsequent phase transformations. Second, the Si-II phase becomes more unstable upon further pressure release and, at a critical pressure, those seeds of high-pressure phases rapidly grow to occupy substantial volumes of the phase transformation region underneath the indenter, leading to pop-out. Fast unloading reduces the nucleation probability of high-pressure phases during early stages of unloading, and also limits the growth of high-pressure phases during subsequent pressure release; thus it leads to the phase transformation from Si-II to *a*-Si gradually and an elbow appears. The nucleation and growth mechanism mentioned above gives a reasonable model for understanding the formation of high-pressure phases during unloading.

However, the effect of the loading rate is still not clear. In this study, the results in figures 1(d) and (a) are similar, indicating that the loading rate has less impact on phase transformations in single-crystal silicon. Even though the loading rate is very high, it does not affect the formation of

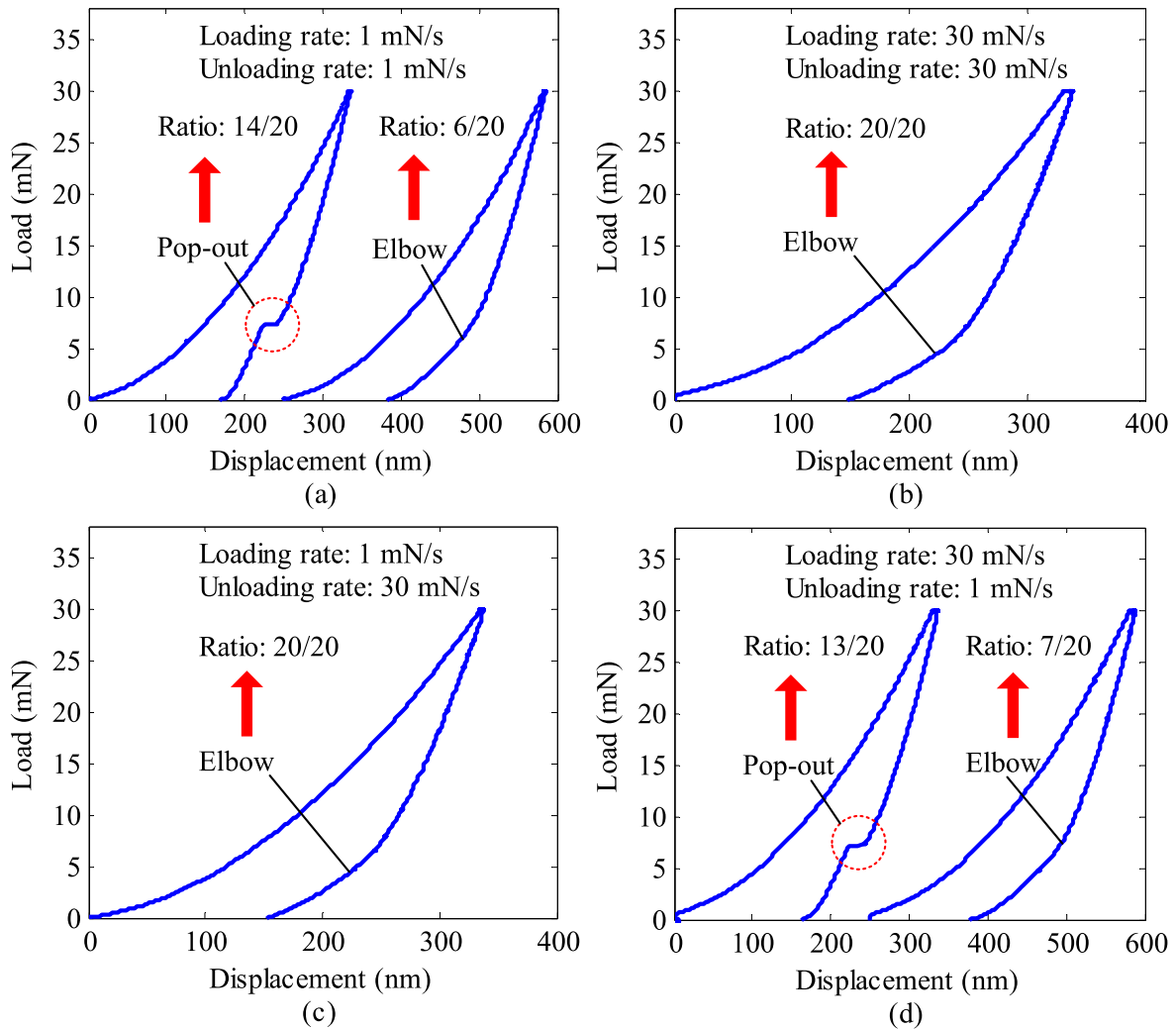


Figure 1. Statistical results of nanoindentation in single-crystal silicon under a maximum indentation load of 30 mN but different loading/unloading rates: (a) loading/unloading rate 1 mN s^{-1} , (b) loading/unloading rate 30 mN s^{-1} , (c) loading rate 1 mN s^{-1} , unloading rate 30 mN s^{-1} , and (d) loading rate 30 mN s^{-1} , unloading rate 1 mN s^{-1} .

high-pressure phases given a low unloading rate. For the purpose of rapid formation of high-pressure phases, fast loading and slow unloading are preferable.

Figure 2 gives statistical results of nanoindentation in single-crystal silicon under a higher maximum indentation load (60 mN), using a high loading rate of 30 mN s^{-1} and a low unloading rate of 1 mN s^{-1} . Under these conditions, all 20 tests exhibit obvious pop-outs. A higher indentation load induces a larger deformation region underneath the indenter, which increases the possibility of random nucleation of high-pressure phases during unloading and thus promotes pop-out.

From figures 1 and 2, it is made clear that a large maximum indentation load, a high loading rate, and a low unloading rate are suitable conditions for the efficient formation of high-pressure phases during nanoindentation. The next questions are whether the formation efficiency of high-pressure Si phases can be further improved and whether high-pressure phases can be formed under a high unloading rate.

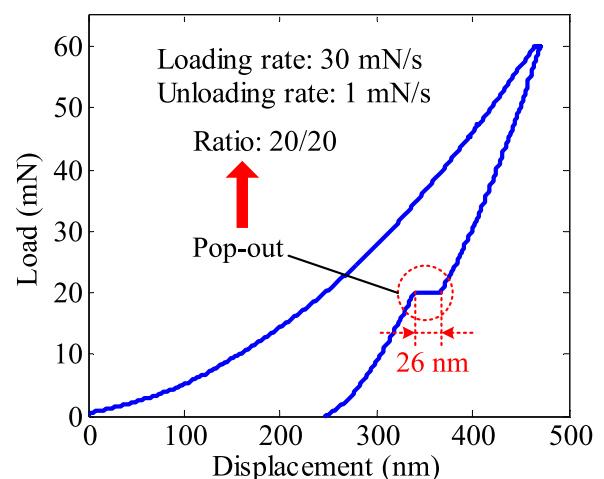


Figure 2. Statistical results of nanoindentation in single-crystal silicon under a maximum indentation load of 60 mN, a loading rate of 30 mN s^{-1} , and an unloading rate of 1 mN s^{-1} .

The nucleation and growth mechanism suggest that fast unloading lowers the possibility of random nucleation of high-pressure phases and also limits their growth during the subsequent pressure release [32]. From this point of view, we may presume that if an intermediate holding stage is provided for nucleation and growth of high-pressure phases during unloading under a high loading/unloading rate, phase transformations from the Si-II phase to high-pressure phases may be realized. Based on this idea, unloading tests were implemented by introducing intermediate holding stages at loads of 8 and 16 mN for the maximum indentation loads of 30 and 60 mN, respectively. The holding time was 20 s. In these tests, the loading rate and unloading rate were both 30 mN s^{-1} . Statistical results are presented in figure 3.

In figures 3(b), (d), and (e), time begins from the indentation initiation. Thus, the intermediate holding stage begins at 2.7 s and finishes at 22.7 s in figure 3(b) for the maximum indentation load of 30 mN, while the start and end times are 4.5 and 24.5 s for the maximum indentation load of 60 mN in figure 3(d). In figures 3(a) and (b), under the maximum indentation load of 30 mN and a loading/unloading rate of 30 mN s^{-1} , six pop-outs occur during the intermediate holding stages and the displacement change during the pop-out is about 18 nm; the other 14 tests only show creep behaviors resulting from gradual elastic recovery of the deformation region underneath the indenter. In figure 3(c), under the maximum indentation load of 60 mN, pop-out appears 16 times during the intermediate holding stages and 2 times before holding in the 20 tests. Only 2 tests show no pop-out. Furthermore, the displacement change in this case is about 26 nm as shown in figure 3(d), greater than that for 30 mN, indicating a larger phase transformation volume underneath the indenter, and the same as that under complete unloading for 60 mN in figure 2. Figure 3(e) illustrates statistical results of occurrence times for the pop-out corresponding to the experimental conditions in figure 3(c). It is obvious that most of the pop-outs occur in the early stages (4.5 s \sim 10 s) of the intermediate holding stages, which means that the intermediate holding time can be further shortened. The results in figure 3 indicate that efficient formation of high-pressure phases can be realized by introducing an intermediate holding stage during fast unloading. Comparing figures 3(c) and 2, even introducing an intermediate holding stage for fast unloading, the total indentation time is still ~ 38 s shorter than that taken in slow unloading. Furthermore, the same volumes of high-pressure phases are induced under these two conditions because the same displacement change appears during pop-outs in figures 3(d) and 2.

To determine whether or not pop-outs occurring at different times lead to the same residual phases, Raman spectra of the residual indents were measured. Figure 4(a) gives a load-displacement curve where the pop-out occurs during the intermediate holding stage in unloading, and figure 4(b) gives a complete load-displacement curve with a pop-out during unloading without intermediate holding. Raman spectra corresponding to the residual indents in figures 4(a) and (b) are presented in figures 4(d) and (e) respectively. For comparison,

a Raman spectrum of the pristine silicon is shown in figure 4(c). Compared with the pristine silicon, very similar new peaks at ~ 169 , 186, 353, 376, 386, 397, 437, and 490 cm^{-1} are observed in both figures 4(d) and (e). According to references [25, 35, 36], peaks at ~ 186 , 353, 376, and 397 cm^{-1} correspond to the Si-XII phase and peaks at ~ 169 , 386, 437, 490 cm^{-1} correspond to the Si-III phase. The results shown in figure 4 demonstrate that the dominant end phases in the residual indents after the pop-outs are the same, namely Si-XII/Si-III phases, independent of the position of the pop-out.

Although the dominant end phases corresponding to the pop-out occurring during the intermediate holding stage in unloading are the same as those corresponding to the pop-out occurring during a complete unloading process, their phase transformation processes may be different because the unloading rate is very different. For a low unloading rate of 1 mN s^{-1} in figure 4(b), initial nucleation of high-pressure phases and subsequent growth upon further pressure release could readily occur according to the crystal nucleation and growth mechanism in [32, 34]. However, for a fast unloading rate of 30 mN s^{-1} in figure 4(a), initial nucleation of high-pressure phases during early stages of unloading could be hindered, and thus the kinetics of phase transformation and the formation processes of high-pressure phases may be different [37]. In this case, an intermediate phase [38], the Ostwald ripening stage [37], and other processes [39, 40] may occur. Hence, phase transformation processes for the pop-out occurring during the intermediate holding stage in unloading at a fast unloading rate and their difference from the pop-out occurring during a complete unloading process at a low unloading rate need further investigation. Considering that these issues are very complex and more experiments are required, such as experiments by *in situ* Raman microspectroscopy, cross-sectional transmission electron microscopy (XTEM), or *in situ* electrical characterization, we will discuss them in another paper in the future.

4. Conclusions

In this paper, key factors affecting the formation of high-pressure phases of silicon in nanoindentation were investigated by comparative experiments. The results show that the loading rate has less impact on the formation of high-pressure phases. A large maximum indentation load, a high loading rate and a low unloading rate are suitable for efficient formation of high-pressure phases in conventional nanoindentation tests. To improve the efficiency of formation of high-pressure phases, fast unloading was attempted by introducing an intermediate holding stage, and high-pressure phases were successfully formed. The Raman spectra results confirm that the dominant end phases are a mixture of Si-XII/Si-III phases, and that the intermediate holding does not change the end phases provided pop-out has occurred. The findings from this study provide useful information for developing future mechanical manufacturing processes to produce high-pressure phases of silicon.

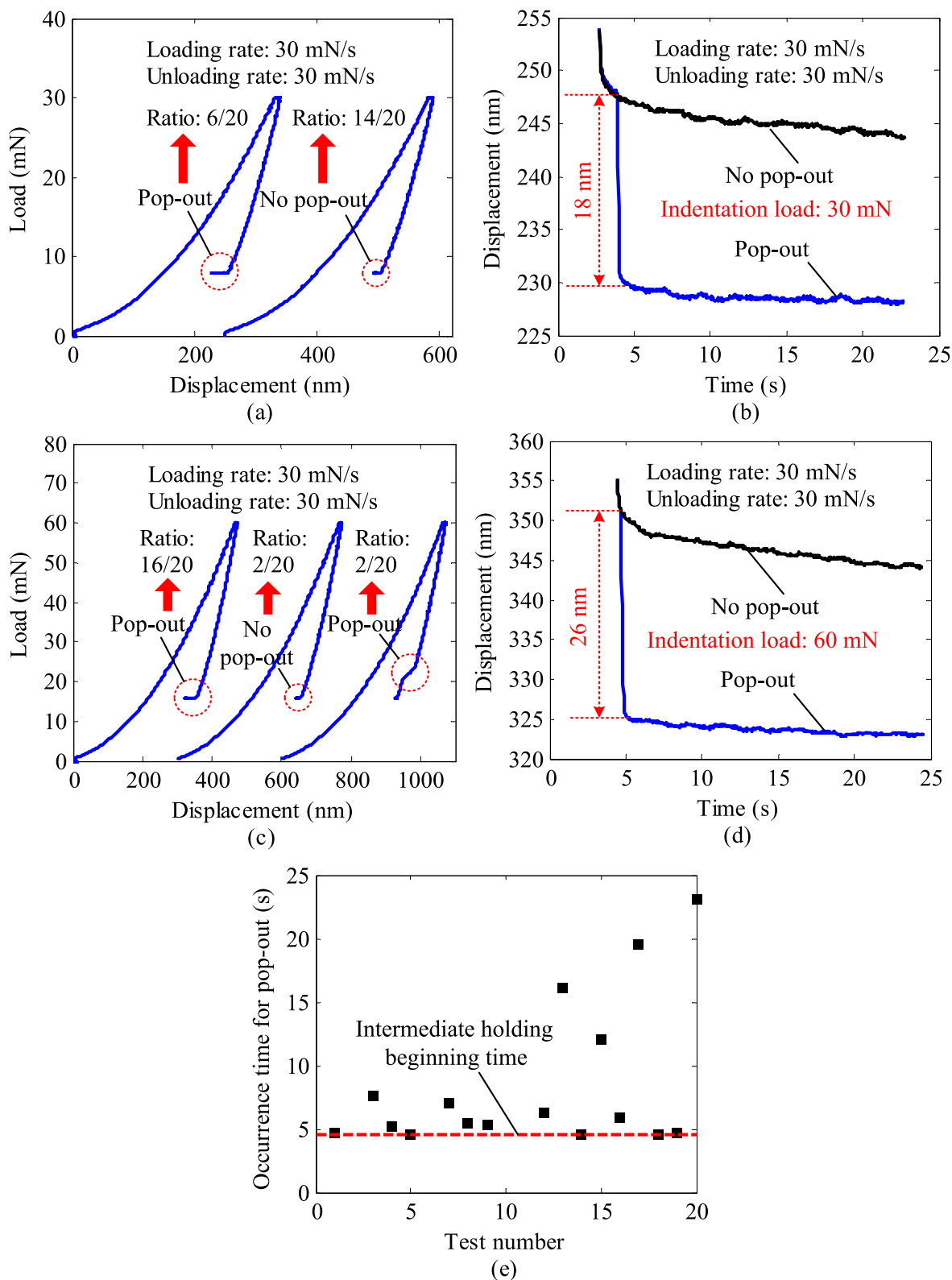


Figure 3. (a) Statistical results of nanoindentation under a maximum indentation load of 30 mN, loading/unloading rates of 30 mN s^{-1} and an intermediate holding at 8 mN; (b) displacement-time curves corresponding to load-displacement curves in figure 3(a); (c) statistical results of nanoindentation under a maximum indentation load of 60 mN, loading/unloading rates of 30 mN s^{-1} and an intermediate holding at 16 mN; (d) displacement-time curves corresponding to load-displacement curves in figure 3(c); and (e) statistical results of occurrence time for the pop-out corresponding to experimental conditions in figure 3(c). In figures 3(b), (d) and (e), time begins from the indentation initiation.

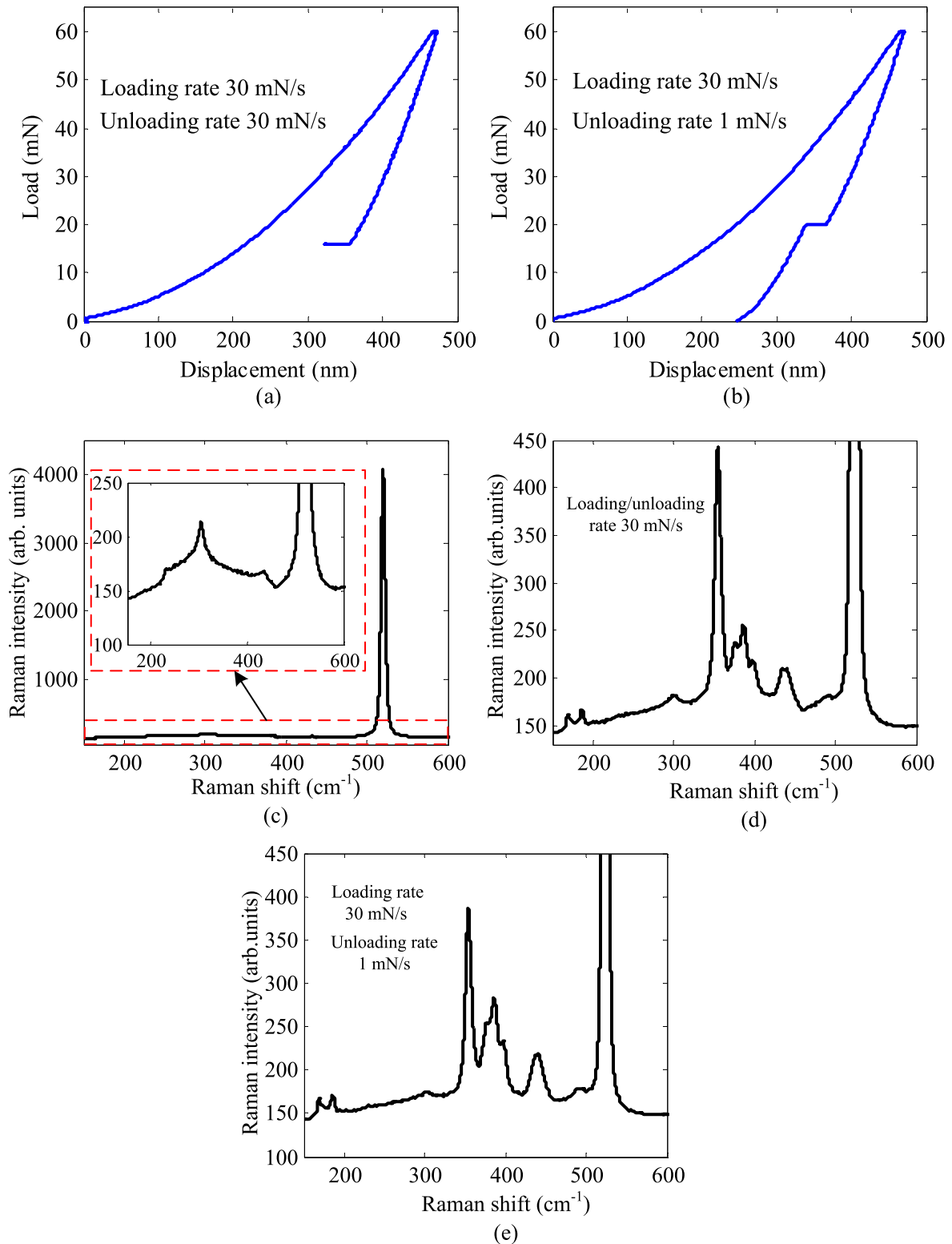


Figure 4. (a) A load-displacement curve with a pop-out occurring during an intermediate holding stage in unloading; (b) a complete load-displacement curve with a pop-out during unloading without intermediate holding; (c) Raman spectrum of the pristine silicon; (d) Raman spectrum corresponding to the residual indent in figure 4(a); (e) Raman spectrum corresponding to the residual indent in figure 4(b).

Acknowledgments

H H is an International Research Fellow of the Japan Society for the Promotion of Science (JSPS). This study has been financially supported by Grant-in-Aid for JSPS Fellows (Grant No. 26-04048) and Grant-in-Aid for Exploratory Research (Grant No. 15K13838).

References

- [1] Mcmahon M I and Nelmes R J 1993 *Phys. Rev. B* **47** 8337
- [2] Voronin G A, Pantea C, Zerda T W, Wang L and Zhao Y 2003 *Phys. Rev. B* **68** 020102
- [3] Shchennikov V V, Shchennikov V V, Streltsov S V, Korobeynikov I V and Ovsyannikov S V 2013 *J. Electron. Mater.* **42** 2249
- [4] Bradby J E, Williams J S, Wong-Leung J, Swain M V and Munroe P 2001 *J. Mater. Res.* **16** 1500
- [5] Gogotsi Y, Miletich T, Gardner M and Rosenberg M 1999 *Rev. Sci. Instrum.* **70** 4612
- [6] Crain J, Ackland G J, Maclean J R, Piltz R O, Hatton P D and Pawley G S 1994 *Phys. Rev. B* **50** 13043
- [7] Auckland G J 2001 *Rep. Prog. Phys.* **64** 483
- [8] Piltz R O, Maclean J R, Clark S J, Ackland G J, Hatton P D and Crain J 1995 *Phys. Rev. B* **52** 4072
- [9] Kailer A, Gogotsi Y G and Nickel K G 1997 *J. Appl. Phys.* **81** 3057
- [10] Zeng Z D, Zeng Q S, Mao W L and Qu S X 2014 *J. Appl. Phys.* **115** 103514
- [11] Domnich V and Gogotsi Y 2002 *Rev. Adv. Mater. Sci.* **3** 1
- [12] Mujica A, Rubio A, Munoz A and Needs R J 2003 *Rev. Mod. Phys.* **75** 863
- [13] Domnich V, Gogotsi Y and Dub S 2000 *Appl. Phys. Lett.* **76** 2214
- [14] Yan J W, Syoji K, Kuriyagawa T and Suzuki H 2002 *J. Mater. Process. Technol.* **121** 363
- [15] Malone B D, Sau J D and Cohen M L 2008 *Phys. Rev. B* **78** 035210
- [16] Malone B D, Sau J D and Cohen M L 2008 *Phys. Rev. B* **78** 161202
- [17] Youn S W and Kang C G 2004 *Scr. Mater.* **50** 105
- [18] Mignot J M, Chouteau G and Martinez G 1986 *Phys. Rev. B* **34** 3150
- [19] Besson J M, Mokhtari E H, Gonzalez J and Weill G 1987 *Phys. Rev. Lett.* **59** 473
- [20] Wippermann S, Voros M, Rocca D, Gali A, Zimanyi G and Galli G 2013 *Phys. Rev. Lett.* **110** 046804
- [21] Juliano T, Gogotsi Y and Domnich V 2003 *J. Mater. Res.* **18** 1192
- [22] Jang J I, Lance M J, Wen S Q, Tsui T Y and Pharr G M 2005 *Acta Mater.* **53** 1759
- [23] Yan J W, Takahashi H, Gai X H, Harada H, Tamaki J and Kuriyagawa T 2006 *Mater. Sci. Eng. A* **423** 19
- [24] Kiriya T, Harada H and Yan J W 2009 *Semicond. Sci. Technol.* **24** 025014
- [25] Jasinevicius R G, Duducha J G and Pizani P S 2008 *Mater. Lett.* **62** 812
- [26] Zarudi I, Zhang L C and Swain M V 2004 *Proc. Inst. Mech. Eng. C* **218** 591
- [27] Chang L and Zhang L C 2009 *Acta Mater.* **57** 2148
- [28] Juliano T, Domnich V and Gogotsi Y 2004 *J. Mater. Res.* **19** 3099
- [29] Mann A B 2005 Nanomechanical properties of solid surfaces and thin films *Nanotribology and Nanomechanics: An Introduction* ed B Bhushan (Berlin: Springer) ch 12, pp 575–622
- [30] Gerbig Y B, Stranick S J and Cook R F 2011 *Phys. Rev. B* **83** 205209
- [31] Zarudi I, Zou J and Zhang L C 2003 *Appl. Phys. Lett.* **82** 874
- [32] Ruffell S, Bradby J E, Williams J S and Munroe P 2007 *J. Appl. Phys.* **102** 063521
- [33] Ruffell S, Bradby J E, Williams J S and Warren O L 2007 *J. Mater. Res.* **22** 578
- [34] Fujisawa N, Ruffell S, Bradby J E, Williams J S, Haberl B and Warren O L 2009 *J. Appl. Phys.* **105** 106111
- [35] Jasinevicius R G, Duduch J G and Pizani P S 2007 *Semicond. Sci. Technol.* **22** 561
- [36] Gogotsi Y, Baek C and Kirscht F 1999 *Semicond. Sci. Technol.* **14** 936
- [37] Slezov V V 2009 *Kinetics of First-order Phase Transitions* (Weinheim: Wiley)
- [38] Kukushkin S A and Osipov A V 2014 *Phys. Solid State* **56** 792
- [39] Kukushkin S A 2005 *J. Appl. Phys.* **98** 033503
- [40] Kukushkin S A and Osipov A V 1998 *Phys.-Usp.* **41** 983